Anomeric Effect in Purine Nucleosides. Evaluation of the Steric Effect of a Purinic Aglycon from the Pseudorotational Equilibrium of Cyclopentane in Carbocyclic *C*-Nucleoside **1**

Matjaž Polak, Barbara Mohar, Jože Kobe, and Janez Plavec*

Contribution from the National Institute of Chemistry, Hajdrihova 19, SI-1115 Ljubljana, Slovenia

Received July 21, 1997

Abstract: A variable temperature 600 MHz ^{1}H NMR conformational analysis of $^3J_{HH}$ coupling constants in pyrazolo[4,3-*c*]pyridine *carbaribo*-*C*-nucleoside **1** in D_2O has shown that the carbocyclic nucleoside analogues in which the furanose ring is replaced by a cyclopentane are involved in a two-state N ⇄ S (north ⇄ south) pseudorotational equilibrium, which is in the case of **1** strongly biased toward an S-type conformation (P = 137°, Ψ_m = 37°, 90% at 298 K). The van't Hoff analysis of the population changes with temperature has shown that the pseudorotational equilibrium in **1** is driven toward S by a $\Delta H°$ of −11.6 kJ mol^{-1}. The two-state dynamic equilibrium is supported by ab initio calculations at HF, DFT, and MP2 levels which showed two energy wells in the N and S regions of conformational space. At the MP2/6-31(d) level the S-type conformer is preferred by 10.9 kJ mol^{-1} over the local minimum in the N region of conformational space, which is in excellent agreement with our experimental value from the conformational analysis of $^3J_{HH}$. The N and S energy minima are separated with the energy barrier of 24.0 kJ mol^{-1} at the MP2 level, which suggests a rapid exchange on the NMR time scale between the interconverting conformers. The experimental quantitative estimate of $\Delta H°_{steric}$ (−12.0 kJ mol^{-1}) of the pyrazolopyridine moiety, which has been assumed to be isosteric with the purine moiety, has been used to calculate the energetic strengths of the O4′−C1′−N9 anomeric effects of adenine and guanine in *N*-nucleosides: 16.4 kJ mol^{-1} in ddA and ddG, 14.7 kJ mol^{-1} in dA, 16.4 kJ mol^{-1} in dG, 13.9 kJ mol^{-1} in A, and 15.3 kJ mol^{-1} in G.

Introduction

The D-ribofuranose or 2′-deoxy-D-ribofuranose moieties in natural nucleosides are capable of adopting a variety of distinct conformations, which has direct influence on the conformation of the backbone chain in DNA and RNA.[1] From numerous X-ray studies and a large collection of NMR data, it is well established that the sugar moieties of nucleos(t)ides are involved in a two-state conformational equilibrium between two distinctly identifiable north (N) and south (S) conformations which are dynamically interconverting in solution.[1−3] The two-state N ⇄ S pseudorotational equilibrium in solution is controlled by the competing anomeric and gauche effects.[3] The 2′-OH and 3′-OH groups drive the equilibrium through the tendency to adopt a gauche arrangement of O−C−C−O fragments with O4′−C1′/C4′ bonds. The heterocyclic bases in *N*-nucleosides drive the two-state N ⇄ S pseudorotational equilibrium of the constituent β-D-pentofuranosyl moieties by two counteracting contributions from (i) the anomeric effect and (ii) the inherent steric effect of the nucleobase. The anomeric effect describes the empirical observation of a preference for electronegative exocyclic substituents to occupy the pseudoaxial over the pseudoequatorial position at the anomeric carbon.[4] Whereas there is still some dispute as to the origin of the anomeric effect, clear experimental evidence exists that its strength is closely related to the electronic nature of the aglycon.[3] For example, the protonation of the nucleobase facilitates the interaction between lone pair orbitals of O4′ and orbitals of the glycosidic bond, which results in the increased preference for N-type conformers.[3c] On the other hand, the steric effect, which opposes the anomeric effect by its tendency to take up the pseudoequatorial orientation and drives N ⇄ S pseudorotational equilibrium toward S-type conformers, is determined by the shape and the size of the substituent at the anomeric carbon. The problem of separating the two contributions which counteract in the drive of N ⇄ S pseudorotational equilibrium remains. Studies on the purine *C*-nucleosides have shown that their N ⇄ S pseudorotational equilibria are characterized by a predominant population of S-type conformers where the nucleobase is in the pseudoequatorial orientation.[3b] A recent pD-dependent study[5] has provided the evidence of the tunable anomeric effect in those *C*-nucleosides, indicating that there exist n(O4′) → $\sigma^*_{C1'-Csp2}$ interactions which drive the pseudorotational equilibrium toward the north conformation. This places some ambiguity as to whether deprotonated heterocyclic moieties in *C*-nucleosides at very high pD really exert a drive on N ⇄ S equilibrium exclusively through the steric bulk and are therefore a proper reference for the evaluation of steric effect in purine nucleosides.

(1) Saenger, W. *Principles of Nucleic Acid Structure*, Springer-Verlag: Berlin, 1988.

(2) Altona, C.; Sundaralingam, M. *J. Am. Chem. Soc.* **1972**, *94*, 8205; **1973**, *95*, 2333.

(3) (a) Plavec, J.; Tong, W.; Chattopadhyaya, J. *J. Am. Chem. Soc.* **1993**, *115*, 9734. (b) Thibaudeau, C.; Plavec, J.; Chattopadhyaya, J. *J. Am. Chem. Soc.* **1994**, *116*, 8033. (c) Thibaudeau, C.; Plavec, J.; Chattopadhyaya, J. *J. Org. Chem.* **1996**, *61*, 266.

(4) (a) Kirby, A. J.; Williams, N. H. *The Anomeric Effect and Associated Stereoelectronic Effects*; ACS: Washington, DC, 1993; p 55. (b) Juaristi, E.; Cuevas, G. *Tetrahedron* **1992**, *48*, 5019. (c) Tvaroška, I.; Bleha, T. *Adv. Carbohydr. Chem. Biochem.* **1989**, *47*, 45.

(5) Luyten, I.; Thibaudeau, C.; Sandstrom, A.; Chattopadhyaya, J. *Tetrahedron* **1997**, *53*, 6433.

S0002-7863(97)02433-5 CCC: $15.00
Published on Web 03/07/1998

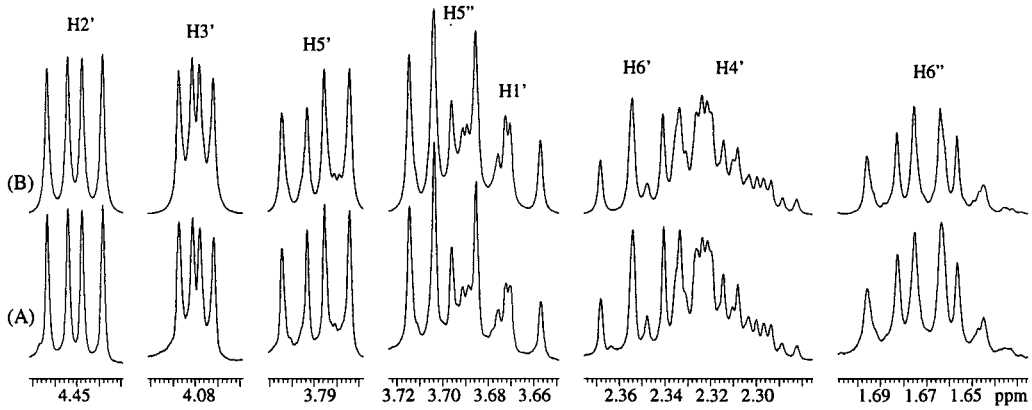

Figure 1. ^{1}H NMR (600 MHz) spectra of **1** in D_2O at 308 K: (A) experimental 1D absorption spectrum; (B) simulated spectrum.

We have initiated a conformational study of carbocyclic *C*-nucleoside analogues in which the furanose ring is replaced by a cyclopentane. A pyrazolo[4,3-*c*]pyridine *carbaribo-C*-nucleoside, **1**,[6] has been chosen as a model compound to evaluate for the first time the pseudorotational equilibrium of the cyclopentane ring in carbocyclic nucleoside analogues.

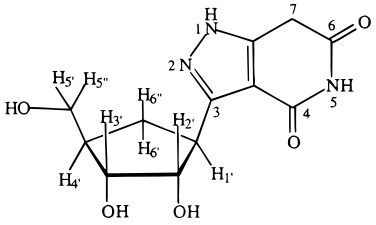

1

The conformational study of nucleoside analogue **1** has been performed with the following objectives in mind: (1) First, to examine if the cyclopentane ring in **1** adopts a two-state N ⇄ S pseudorotational equilibrium. Simple model building shows that the [O2′−C2′−C3′−O3′] torsion angle is in a highly unfavored cis arrangement at $P = 90°$ and 270°, but it takes up a gauche orientation in N- and S-type conformers which should therefore be preferred. To obtain complementary information, we have turned to X-ray crystallography and ab initio calculations. X-ray crystal structure data on carbocyclic nucleosides are too scarce to allow any conclusions on the conformational equilibria of the constituent cyclopentane.[7] The pseudorotational energy profile at the HF/3-21G level showed two energy wells in the N and S regions of conformational space for **1** with an energy barrier which suggests the occurrence of two conformers in rapid equilibrium on the NMR time scale (vide infra). (2) Second, the sensitivity of the experimental $^3J_{HH}$ to the change of temperature indicates the role of enthalpy on the drive of N ⇄ S pseudorotational equilibrium in **1**. A quantitative evaluation of $\Delta H°_{steric}$ of the purine-type aglycon through a simple comparison of the respective $\Delta H°$ values of the N ⇄ S pseudorotational equilibrium of our model compound **1** with $\Delta H°$ of the corresponding purine *N*-nucleosides has given us a direct measure of the energetic strength of the O4′−C1′−N9 anomeric effect in adenine and guanine nucleosides. The underlying assumption is that the pyrazolopyridine moiety is isosteric with the purine moiety. (3) Third, the fact that carbocyclic nucleoside analogues are involved in a common N ⇄ S pseudorotational equilibrium presumably due to polar 2′- and 3′-substituents (i.e., [X2′−C2′−C3′−X3′] gauche effect, where X could be OH, F, NO_2, phosphate, or another electron-withdrawing group) and not by fused ring(s)[8] has a direct impact on their ability to serve as substrates for certain enzymes and on the binding of single-stranded oligonucleotides with carbocyclic nucleotides to a specific RNA target ("antisense approach").[9]

Procedures

The analysis of the solution conformation of the cyclopentane ring in **1** is based on seven coupling constants ($^3J_{1'2'}$, $^3J_{1'6'}$, $^3J_{1'6''}$, $^3J_{2'3'}$, $^3J_{3'4'}$, $^3J_{4'6'}$, and $^3J_{4'6''}$) acquired at nine temperatures in the range from 275 to 348 K. The precise values for proton−proton coupling constants from a complex eight-spin system and chemical shifts were obtained through the simulation and iteration procedure (see Figure 1). The resulting vicinal coupling constants $^3J_{HH}$ are presented in Table 1.

We attempted to describe the experimental $^3J_{HH}$ data in terms of a two-state equilibrium as is normally done for ribose or 2′-deoxyribose rings. Note that the two-state model for cyclopentane in **1** is supported by our ab initio calculations. The analysis of $^3J_{HH}$ consists of three essential translation steps. The first step translates coupling constants of vicinal protons to proton−proton torsion angles and is covered by the generalized Karplus−Altona equation.[10] We have taken particular care to account for the substitution of O4′ in the natural pentofuranosyl moiety with a CH_2 group in cyclopentane. In addition, the correction for the Barfield transmission effect[10g,h] has been used to account for a

(6) The synthesis of 3-[(1*S*,2*S*,3*R*,4*R*)-2,3-dihydroxy-4-(hydroxymethyl)-cyclopentyl]-1*H*-pyrazolo[4, 3-*c*]pyridine-4,6(5*H*,7*H*)-dione (**1**) is described in Mohar, B.; Kobe J. *Nucleosides Nucleotides* **1997**, *16*, 1427.

(7) (a) We have performed a search of the Cambridge Structural Database with the query for a cyclopentane which is substituted at positions 1 and 3 with carbon or nitrogen atoms. We discarded the hits in which the cyclopentane is fused to another ring, because it is well-known that the size of the fused ring has a great influence on the puckering. Our search ended up with two nucleoside analogues with refcodes ARSTMC10, $P = 89.2°$, $\Psi_m = 40.7°$ (Kishi, T.; Muroi, M.; Kusaka, T.; Nishikawa, M.; Kamiya, K.; Mizuno, K. *Chem. Pharm. Bull.* **1972**, *20*, 940) and VIKFEA, $P = 118.6°$, $\Psi_m = 41.2°$ (Kalman, A.; Koritsanszky, T.; Beres, J.; Sagi, G. *Nucleosides Nucleotides* **1990**, *9*, 235). (b) Sundaralingam, M. Private communication. X-ray crystal structures of several carbocyclic nucleoside analogues (coordinates not deposited in CSDB) were determined, and they exhibit normal N- or S-type sugar conformations.

(8) Ezzitouni, A.; Marquez, V. E. *J. Chem. Soc., Perkin Trans. 1* **1997**, 1073.

(9) Portmann, S.; Altmann, K.-H.; Reynes, N.; Egli, M. *J. Am. Chem. Soc.* **1997**, *119*, 2396.

(10) (a) Altona, C.; Francke, R.; de Haan, R.; Ippel, J. H.; Daalmans, G. J.; Hoekzema, A. J. A. W.; van Wijk, J. *Magn. Reson. Chem.* **1994**, *32*, 670. (b) Donders, L. A.; de Leeuw, F. A. A. M.; Altona, C. *Magn. Reson. Chem.* **1989**, *27*, 556. (c) Altona, C.; Ippel, J. H.; Westra Hoekzema, A. J. A.; Erkelens, C.; Groesbeek, M.; Donders, L. A. *Magn. Reson. Chem.* **1989**, *27*, 564. (d) Haasnoot, C. A. G.; de Leeuw, F. A. A. M.; de Leeuw, H. P. M.; Altona, C. *Org. Magn. Reson.* **1981**, *15*, 43. (e) Haasnoot, C. A. G.; de Leeuw, F. A. A. M.; Altona, C. *Tetrahedron* **1980**, *36*, 2783. (f) de Leeuw, F. A. A. M.; Altona, C. *J. Comput. Chem.* **1983**, *4*, 428. (g) de Leeuw, F. A. A. M.; van Beuzekom, A. A.; Altona, C. *J. Comput. Chem.* **1983**, *4*, 438. (h) Marshall, J. L.; Walter, S. R.; Barfield, M.; Marchand, A. P.; Marchand, N. W.; Segre, A. L. *Tetrahedron* **1976**, *32*, 537.

Table 1. Evaluation of the Conformational Equilibria in **1** from the Temperature Variation of the Experimental $^3J_{HH}$ Coupling Constants

	N ⇄ S pseudorotational equilibrium of cyclopentane[a]								conformational equilibrium across the C4′−C5′ bond[c]				
T (K)	$^3J_{1'2'}$	$^3J_{1'6'}$	$^3J_{1'6''}$	$^3J_{2'3'}$	$^3J_{3'4'}$	$^3J_{4'6'}$	$^3J_{4'6''}$	% S[b]	$^3J_{4'5'}$	$^3J_{4'5''}$	% γ^+	% γ^t	% γ^-
275	9.6	8.2	11.3	5.4	3.2	8.9	8.1	93.8	6.8	6.6	17.0	39.9	43.1
278	9.5	8.2	11.3	5.4	3.3	8.9	8.2	92.6	6.8	6.6	17.0	39.9	43.1
288	9.5	8.2	11.3	5.4	3.4	8.9	8.4	91.8	6.8	6.6	17.0	39.9	43.1
298	9.4	8.2	11.3	5.5	3.6	8.8	8.6	90.0	6.8	6.7	16.1	41.0	42.9
308	9.3	8.1	11.3	5.5	3.7	8.7	8.7	88.9	6.8	6.7	16.1	41.0	42.9
318	9.1	8.2	11.3	5.5	3.8	8.6	8.7	87.2	6.6	6.7	17.8	41.5	40.7
328	9.1	8.2	11.3	5.6	4.0	8.6	8.9	86.0	6.7	6.8	16.0	42.3	41.6
338	9.0	8.2	11.2	5.6	4.2	8.5	9.0	84.0	6.7	6.8	16.0	42.3	41.6
348	8.9	8.2	11.2	5.6	4.2	8.5	9.0	83.5	6.6	6.8	16.9	42.6	40.5

[a] $^3J_{HH}$ values (Hz, ±0.1 Hz) have been extracted from 1D ^{1}H NMR spectra recorded at 600 MHz in D_2O. All coupling constants and chemical shifts have been carefully checked with simulation. δ (D_2O, 298 K, TMSPA = 0 ppm): 4.45 (H2′), 4.07 (H3′), 3.78 (H5′), 3.69 (H5″), 3.67 (H1′), 2.33 (H6′), 2.30 (H4′), 1.67 (H6″) ppm. $^2J_{6'6''} = -13.1$ Hz and $^2J_{5'5''} = -11.1$ Hz. [b] The PSEUROT program[10f] has been used to calculate the population of the major S conformer ($P_S = 137°$, $\Psi_m^S = 37°$), which is in equilibrium with the N conformer ($P_N = 28°$, $\Psi_m^N = 43°$). [c] The experimental $^3J_{4'5'}$ and $^3J_{4'5''}$ coupling constants have been interpreted in terms of the conformational equilibrium between three staggered conformers.

cos^2 dependence of cisoidal $^3J_{1'6'}$, $^3J_{2'3'}$, and $^3J_{4'6'}$ coupling constants upon the phase angle of pseudorotation (P). The second step is the translation of proton−proton torsion angles into the corresponding endocyclic torsion angles and is formulated with the set of linear equations $\Phi_{HH} = A\nu_j + B$. Φ_{HH} is the torsion angle between two vicinal protons and ν_j is the corresponding endocyclic torsion angle.[11] Parameters A and B are corrections for the nonideality of Newman projection symmetry and have been determined for **1** with the use of ab initio optimized geometries at the HF/3-21G level. A set of nineteen ab initio optimized structures with the phase angle of pseudorotation incremented in ca. 20° steps from 0° to 340° has been used to obtain nineteen sets of seven proton−proton torsion angles and the five corresponding endocyclic torsion angles. The A and B parameters were calculated with the use of linear regression, and the resulting linear equations are as follows: $\Phi_{1'6'} = 1.081\nu_0 - 3.62°$, $\Phi_{1'6''} = 1.072\nu_0 - 124.60°$, $\Phi_{1'2'} = 1.128\nu_1 + 121.95°$, $\Phi_{2'3'} = 1.212\nu_2 - 1.49°$, $\Phi_{3'4'} = 1.149\nu_3 - 121.22°$, $\Phi_{4'6'} = 1.151\nu_4 + 1.83°$, and $\Phi_{4'6''} = 1.147\nu_4 + 122.31°$ (all relations showed the Pearson correlation coefficient higher than 0.997). The third translational step of endocyclic torsion angles into the pseudorotational parameters is described by a simple cosine function, $\nu_j = \Psi_m \cos[P + (j-2)4\pi/5]$, where P is the phase angle of pseudorotation and Ψ_m is the maximum puckering amplitude.[2,11]

Results

Ab initio Evaluation of the Puckering and Pseudorotational Equilibrium of the Cyclopentane Ring in 1. The energetics of the pseudorotational equilibrium of **1** has been examined by ab initio molecular orbital calculations at HF, DFT, and MP2 levels of theory. First, we examined if the cyclopentane ring in **1** adopts a standard two-state N ⇄ S pseudorotational equilibrium characteristic for natural pentofuranosyl nucleosides. A set of 19 conformers, which were chosen in such a way to scan the conformational space from W via N and E to S regions at a maximum puckering amplitude of 40°, was energy optimized at HF/3-21G level. The resulting pseudorotational energy profile at the HF/3-21G level showed two energy wells in the N and S regions of conformational space (see Figure 2). Perusal of the conformational characteristics and respective relative energies, which are given in Table 2, shows that the S-type conformer is preferred by 2.5 kJ mol^{-1} over the N-type conformer at the HF/3-21G level. The two lowest energy conformers at the HF/3-21G level were used as input for completely free optimizations at the HF/6-31G(d) level. The energetic preference for S- over N-type conformers, which were completely freely optimized, has increased to 7.5 kJ mol^{-1} with the 6-31G(d) basis set (Table 2). It is noteworthy that

(11) The endocyclic torsion angles in **1** are defined as follows: $\nu_0 \equiv$ [C4′−C6′−C1′−C2′], $\nu_1 \equiv$ [C6′−C1′−C2′−C3′], $\nu_2 \equiv$ [C1′−C2′−C3′−C4′], $\nu_3 \equiv$ [C2′−C3′−C4′−C6′], and $\nu_4 \equiv$ [C3′−C4′−C6′−C1′].

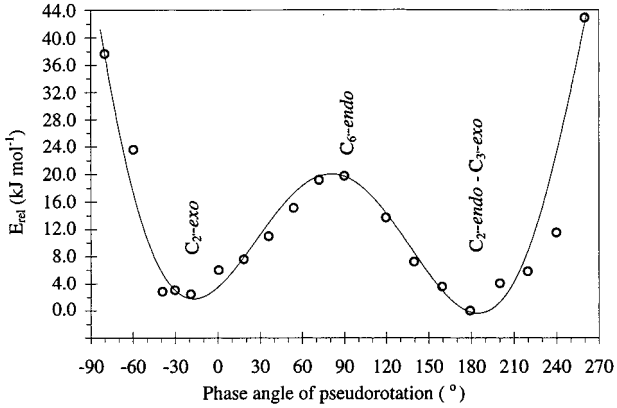

Figure 2. Relative HF/3-21G energy as a function of the phase angle of pseudorotation (P) for **1**. The profile has been obtained through 19 ab initio MO optimizations at the HF/3-21G level by keeping ν_2 and ν_3 frozen at P in the range $-80° < P < +260°$ in 20° steps (Ψ_m = 40°), while all other degrees of freedom were freely optimized. The two conformers in the energy minima were completely freely optimized. Note that the relative energy also reflects the energetic variations due to specific orientations of hydroxy groups, 4′−CH_2OH, and the heterocycle. However, in all 19 structures the following common structural features (completely free during energy optimization) were found: γ-trans, β-trans, $\epsilon_{3'}$-minus, $\epsilon_{2'}$-plus, and anti orientation of the base. The lowest energy conformer, which has been assigned the relative energy (kJ mol^{-1}) of 0.0 is characterized by a HF/3-21G energy of −995.23518 hartrees and has $P = 179.2°$ and $\Psi_m = 40.0°$. The second lowest energy conformer is found at $P = -19.0°$, $\Psi_m = 40.4°$, with a relative energy of 2.5 kJ mol^{-1} above the lowest energy minimum. The two energy minima are separated by a barrier of interconversion of 19.7 kJ mol^{-1} at $P = 90°$, which suggests rapid exchange between N- and S-type pseudorotamers on the NMR time scale.

DFT calculations with the 6-31G(d) basis set showed that the S pseudorotamer has 8.8 kJ mol^{-1} lower energy than the N counterpart (Table 2). The inclusion of electron correlation at the MP2/6-31G(d) level showed a preference of 10.9 kJ mol^{-1} the for S- over N-type pseudorotamer.

The pseudorotational energy profile at the HF/3-21G level which is shown in Figure 2 suggested an energy barrier of 19.7 kJ mol^{-1} in the E region of conformational space at $P = 90°$. When the E pseudorotamer was reoptimized at the HF/6-31G-(d) level, the energy barrier was found to be 16.2 kJ mol^{-1} (Table 2). The MP2 calculation has shown that the E-type conformer is 24.0 kJ mol^{-1} above the minimum in the S region of conformational space (Table 2). In conclusion, the ab initio energy differences between N and S energy minima at the HF, DFT, and MP2 levels of theory are between 2.5 and 10.9 kJ mol^{-1} and are separated with the energy barrier between 14.9

Table 2. Evaluation of the Conformational Equilibria and Energetic Preferences as Obtained by ab Initio MO Calculations on **1**

	3-21G			6-31G(d)				
	P	Ψ_m	E_{rel}-(HF)	*P*	Ψ_m	E_{rel}(HF)	E_{rel}(B3LYP)	E_{rel}(MP2)
north	−19.0	40.4	2.5	30.4	43.1	7.5	8.8	10.9
east	90.0	40.2	19.7	90.0	40.1	16.2	14.9	24.0
south	179.2	40.0	0.0	156.8	42.2	0.0	0.0	0.0

[a] Both N and S energy minima were obtained through energy minimization, where all degrees of freedom were completely freely optimized. In the case of the E pseudorotamer the endocylic torsion angles ν_2 and ν_3 were kept fixed to obtain an estimate of the energy barrier (compare Figure 2). Relative energy (E_{rel}) is given in kJ mol^{-1}. The lowest energy conformer at each level of theory is arbitrarily taken as 0.0 kJ mol^{-1} (see the Supporting Information for the energies in au). *P* and Ψ_m are in degrees. The bond distances and bond angles for the three pseudorotamers of cyclopentane from our ab initio optimized geometries and two X-ray crystal structures[7] are reported in Table 1S in the Supporting Information.

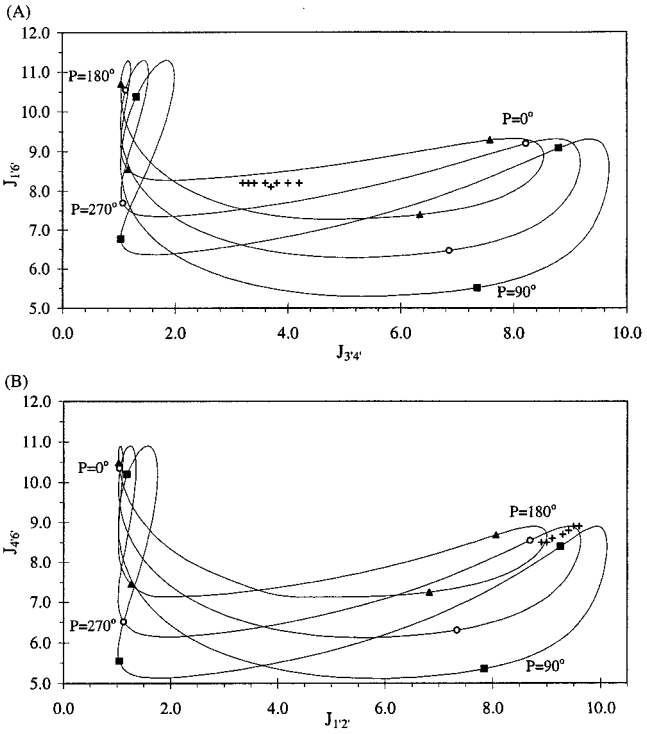

Figure 3. Dependence of $^3J_{HH}$ coupling constants on the phase angle of pseudorotation (*P*) at three fixed puckering amplitudes (Ψ_m). Values for $^3J_{HH}$ were calculated by varying *P* from 0° to 360° via 180° using the six-parameter Karplus type equation[10a] at fixed puckering amplitudes of 32.5° (▲), 37.5° (○), and 42.5° (■). Experimental coupling constants which are shown by a plus sign were obtained from 600 MHz ^{1}H NMR spectra in D_2O at nine different temperatures (Table 1). Both panels A and B show a variation with *P* and Ψ_m of $^3J_{1'6'}$ and $^3J_{4'6'}$ that is not commonly encountered in nucleosides in relation to $^3J_{3'4'}$ and $^3J_{1'2'}$, respectively. The disposition and the alignment of $^3J^{expt}$ suggest in a very descriptive way that cyclopentane in **1** is involved in a highly biased conformational equilibrium of ∼70% (panel A) and ∼90% (panel B) of S-type conformers with $P_S \approx 160°$.

and 24.0 kJ mol^{-1} (Table 2) which suggests a rapid exchange on the NMR time scale between interconverting conformers, resulting in the time-averaged coupling constants and chemical shifts for **1**.

Experimental Evaluation of the N ⇄ S Pseudorotational Equilibrium in Carbocyclic *C*-Nucleoside 1 by NMR. A convenient qualitative representation of the conformational equilibrium of the cyclopentane ring in **1** is given in Figure 3, which shows the variation of vicinal $^3J_{HH}$ with *P* at three fixed values of Ψ_m. Transoidal coupling constants $^3J_{1'2'}$ and $^3J_{3'4'}$ show a large variation of 9 Hz (from 1.1 to 10.1 Hz) over a pseudorotation cycle. The cisoidal couplings $^3J_{1'6'}$ and $^3J_{4'6'}$ show a smaller variation of 6 Hz (from 5.2 to 11.4 Hz). Clearly, the positions of the experimental $^3J_{HH}$ data points in Figure 3 are related to the *J* values in individual conformers and their mole fractions. It is possible to construct conodes through the experimental data points between N- and S-type conformers which clearly show that the conformation of the cyclopentane in **1** is strongly biased toward S-type geometries (Figure 3). The population changes noticeably with the change of temperature, indicating that there is a considerable enthalpy contribution involved in the drive of the N ⇄ S pseudorotational equilibrium of **1**.

In further elaboration of the experimental $^3J_{HH}$ coupling constants we have used the computer program PSEUROT[10f] which calculates the least-squares fit of the five pseudorotational parameters defining the two-state N ⇄ S equilibrium (P_N, Ψ_m^N, P_S, Ψ_m^S, and x_S) to the set of experimental $^3J_{HH}$. The system is overdetermined (4 + 9 unknowns vs 7 × 9 experimental $^3J_{HH}$ couplings) which facilitates our conformational analysis. As our graphical method (Figure 3) indicated a strong bias of N ⇄ S conformational equilibrium in **1** toward S, the pseudorotation parameters of the minor N-type component were constrained to obtain the parameters of the major S-type component (see the Experimental Section for details). After convergence we obtained the best fit (root-mean-square error 0.52 Hz, ΔJ^{max} < 0.8 Hz) for the conformational equilibrium: ($P_N = 28°$, $\Psi_m^N = 43°$) ⇄ ($P_S = 137°$, $\Psi_m^S = 37°$).[12] Note that at 298 K the population of the S-type conformer is 90% (Table 1). The conformational hyperspace attainable to the cyclopentane in **1** has been examined by calculating the root-mean-square error as a function of *P* and Ψ_m in the preferred S range, as well as in the N range. The resulting contour plots (Figure 4) show that **1** is involved in the two-state equilibrium of minor N-type and major S-type conformations (131° < P_S < 140°, 34° < Ψ_m < 38°) with a root-mean-square error below 0.57 Hz and the largest deviation between experimental and calculated $^3J_{HH}$ below 0.9 Hz (Figure 4A). Note that relatively large changes in the values for *P* and Ψ_m in the N region of conformational space are consistent with the experimental $^3J_{HH}$ data (Figure 4B). The populations of individual conformers at various temperatures (Table 1) have been used to calculate the enthalpy and entropy of the N ⇄ S pseudorotational equilibrium in **1** by making van't Hoff plots. Straight lines were obtained which further support the model of a two-state equilibrium for the cyclopentane ring in **1**. We note that the Pearson correlation coefficients between $\ln(x_S/x_N)$ and the reciprocal of the temperature were higher than 0.993. The value of the enthalpy obtained from the slope was −11.6 kJ mol^{-1} (σ = 1.2). The corresponding entropy value derived from the intercept of the straight line was −20.5 J mol^{-1} K^{-1} (σ = 3.4).

(12) A set of pseudorotational analyses on **1** was performed without the consideration of coupling constants involving H6′ and H6″. The conformational analysis of the three remaining $^3J_{HH}$ values at nine temperatures gave the S-type conformer with $P_S = 127°$ and $\Psi_m^S = 46°$ as the major conformer (94% at 275 K, 83% at 348 K, root-mean-square error <0.09, ΔJ < 0.16 Hz). Note that this puckering mode is very similar to the puckering of the major S-type conformer calculated by the conformational analysis of the complete set of experimental $^3J_{HH}$ coupling constants.

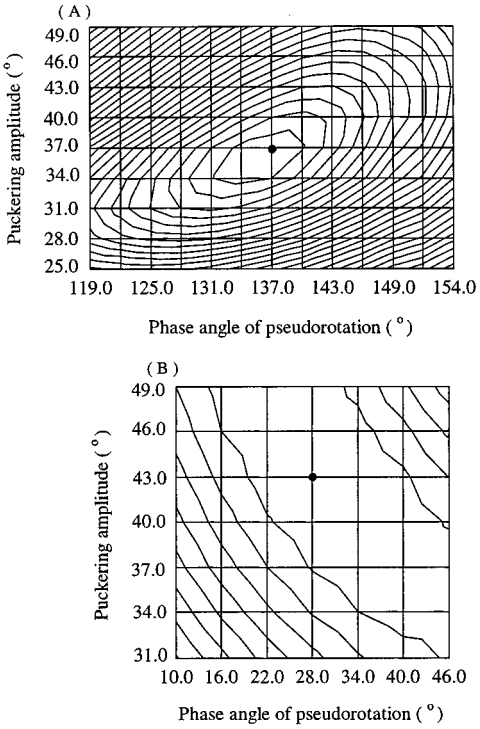

Figure 4. Root-mean-square contours calculated with the computer program PSEUROT[10f] based on the experimental $^3J_{HH}$ (Table 1) by fixing the geometries of the two pseudorotamers participating in the two-state equilibrium for the S (panel A) and N (panel B) regions of conformational space. In panel A the root-mean-square error (contours are spaced by 0.05 Hz; the lowest contour is at 0.57 Hz) was calculated at each point of the grid by systematically changing P and Ψ_m of the major S-type pseudorotamer in 3° steps ($119° \leq P_S \leq 154°$, $25° \leq \Psi_m{}^S \leq 49°$) and keeping the geometry of the minor N-type pseudorotamer fixed at $P_N = 28°$ and $\Psi_m{}^N = 43°$, while populations were optimized. In panel B the root-mean-square error (contours are spaced by 0.01 Hz; the lowest contour is at 0.53 Hz) for the minor N-type pseudorotamer was calculated by systematically changing P and Ψ_m in 6° steps ($10° \leq P_N \leq 46°$, $31° \leq \Psi_m{}^N \leq 49°$) and keeping the geometry of the major S-type pseudorotamer fixed at $P_S = 137°$ and $\Psi_m{}^S = 37°$. The filled dots in both panels A and B represent the best fit between experimental and calculated $^3J_{HH}$ with the root-mean-square error of 0.52 Hz.

Discussion

The heterocyclic base in **1** drives the N ⇄ S pseudorotational equilibrium of the constituent cyclopentane solely through the steric hindrance with the atoms on the β-face of the cyclopentane ring. As the drive of N ⇄ S pseudorotational equilibrium toward N by 4′−CH_2OH is energetically evaluated from $\Delta H°$ (+0.4 kJ mol^{-1})[3a] of abasic (*S*)-tetrahydrofurfuryl alcohol, the $\Delta H°_{steric}$ of the purine-shaped aglycon is −12.0 kJ mol^{-1}. The N ⇄ S pseudorotational equilibrium in 2′,3′-dideoxynucleosides (ddNs) is driven toward N by the anomeric effect of the nucleobase and toward S by its steric effect. The comparison of $\Delta H°$ of ddA ($\Delta H° = 4.8$ kJ mol^{-1})[3] and ddG ($\Delta H° = 4.8$ kJ mol^{-1})[3] with $\Delta H°$ of **1** suggests that anomeric effects of both adenine and guanine are 16.4 kJ mol^{-1}. In doing this, the approximation is made that $\Delta H°_{steric}$ in furanosyl nucleosides is equal to that in their carbocyclic analogues. The N ⇄ S pseudorotational equilibrium is in 2′-deoxynucleosides (dNs) driven toward S by the steric effect of the nucleobase and the gauche effect of the [O3′−C3′−C4′−O4′] fragment, and toward N by the anomeric effect. The comparison of $\Delta H°$ of dA ($\Delta H° = -4.2$ kJ mol^{-1})[3] and dG ($\Delta H° = -2.5$ kJ mol^{-1})[3] with $\Delta H°$ of **1** and considering the drive toward S by the [O3′−C3′−C4′−O4′] gauche effect (−7.3 kJ mol^{-1})[3] suggests that the anomeric effect is 14.7 kJ mol^{-1} for adenine and 16.4 kJ mol^{-1} for guanine in dNs. The comparison of $\Delta H°$ of ribofuranosyl *N*-nucleosides (riboNs), adenosine ($\Delta H° = -4.6$ kJ mol^{-1}),[3] and guanosine ($\Delta H° = -3.2$ kJ mol^{-1})[3] with $\Delta H°$ of similarly 2′- and 3′- substituted **1**, and taking into account the strength of the [O2′−C2′−C1′−N9] gauche effect (−6.9 kJ mol^{-1}),[3] suggests that the anomeric effect is 13.9 kJ mol^{-1} for adenine and 15.3 kJ mol^{-1} for guanine in riboNs. Note that the gauche effects of [O3′−C3′−C4′−O4′] and [O2′−C2′−C1′−O4′] fragments cancel each other in the drive of N ⇄ S pseudorotational equilibrium.[3] The differences in the estimates of O4′−C1′−N9 anomeric effect of adenine and guanine in ddNs, dNs, and riboNs underline the mutual tunability of the forces that drive N ⇄ S pseudorotational equilibrium in nucleosides and nucleotides. It appears that anomeric effects of adenine and guanine are weakened by ca. 0.9 kJ mol^{-1} by the 3′-OH group in dNs, and furthermore by ca. 0.9 kJ mol^{-1} by the 2′-OH in riboNs. The electron-withdrawing hydroxy groups in dNs and riboNs reduce the electron density on O4′ lone pair orbitals, which makes them less available for the interaction with the σ^* orbital of the glycosyl bond. The comparison of the estimates of the anomeric effects for adenine and guanine in ddNs, dNs, and riboNs also suggests that the anomeric effect of adenine is more prone to reduction by 3′-OH and 2′-OH in comparison to guanine. It is interesting to note that the protonation of the nucleobase strengthens more the anomeric effect of guanine ($\Delta\Delta H°_{neutral-protonated} = 4.9$ kJ mol^{-1} for dG and 8.7 kJ mol^{-1} for G, protonated at N7) than the anomeric effect of adenine ($\Delta\Delta H°_{neutral-protonated} = 3.2$ kJ mol^{-1} for dA and 4.2 kJ mol^{-1} for A, protonated at N1).[3c] It should be noted, however, that data on the nucleobase dependent reduction of the anomeric effect by 2′/3′-OH groups is only semiquantitative due to the errors involved in the determination of the populations of the two pseudorotamers at various temperatures. Nevertheless, the above findings represent the necessary experimental data for the (re)parametrization of the force field parameters, which should in addition consider the introduction of the nucleobase specific torsion angle potentials. Further work is in progress to evaluate the differences in C−O, C−N, and C−C bond distances and angles on the steric effect of a nucleobase.

The high preference for the S-type conformation in **1** can possibly explain its lack of antiviral activity in view of results with fused (*N*)- and (*S*)-methanocarbanucleosides,[8] which established a structure−activity relationship for carbocyclic nucleosides with the conformation being locked in the N-type conformation, whereas S-type counterparts are devoid of antiviral activity.

Conclusions

A conformational analysis of $^3J_{HH}$ coupling constants in the complex eight-spin system of pyrazolo[4,3-*c*]pyridine *carbaribo*-*C*-nucleoside **1** in the temperature range from 275 to 348 K in D_2O has shown that the constituent cyclopentane ring is involved in a two-state N ($P = 28°$, $\Psi_m = 43°$) ⇄ S ($P = 137°$, $\Psi_m = 37°$) pseudorotational equilibrium, which is strongly biased toward an S-type conformation. The van't Hoff analysis of the population changes of N and S pseudorotamers with temperature yielded the quantitative estimates for the thermodynamic data on the pseudorotational equilibrium in **1**. The value of $\Delta H°$ (−11.6 kJ mol^{-1}) shows that the pseudoequatorial orientation of the aglycon which is achieved in the S-type conformation is strongly preferred. It is noteworthy that the experimental estimate of $\Delta H°$ for N ⇄ S pseudorotational equilibrium in **1** is in excellent agreement with the ab initio energetic preference

of 10.9 kJ mol^{-1} for the S- over N-type pseudorotamer at the MP2/6-31G(d) level.

A quantitative estimate of $\Delta H°_{steric}$ (−12.0 kJ mol^{-1}) for the purine-shaped aglycon in **1** has been used to evaluate the energetic strength of the O4′−C1′−N9 anomeric effect in adenine and guanine *N*-nucleosides with the assumption that the pyrazolopyridine moiety is isosteric with the purine moiety. The anomeric effect of adenine has been calculated to be 16.4 kJ mol^{-1} in ddA, 14.7 kJ mol^{-1} in dA, and 13.9 kJ mol^{-1} in A, whereas the anomeric effect of guanine is 16.4 kJ mol^{-1} in ddG and in dG and 15.3 kJ mol^{-1} in G.

The interpretation of the experimental $^3J_{4'5'}$ and $^3J_{4'5''}$ coupling constants in terms of the conformational equilibrium between three staggered rotamers has shown that γ^t and γ^- rotamers predominate and are approximately equally populated in **1**, whereas γ^+ is the minor rotamer (Table 1). It is noteworthy that γ^+ and γ^t rotamers are predominant in furanosyl nucleoside analogues due to the gauche effect between C5′−O5′ and C4′−O4′ bonds, which is absent in **1**.

Experimental Section

NMR Spectroscopy. ^{1}H NMR spectra were recorded at 600.113 MHz on a Varian Unity Inova spectrometer and at 299.942 MHz on a Varian Unity Plus NMR spectrometer at the National NMR Center of Slovenia. Spectra were acquired in D_2O (99.9% deuterium) at nine temperatures from 275 to 348 K at neutral pH (the pD* of unbuffered solution was 7.5) and at 10 mM concentration. The sample temperature was controlled to approximately ±0.1 K, with the variable temperature unit being calibrated by a standardized procedure with methanol and ethylene glycol samples. The measurements were performed under the following spectral and processing conditions: 7.5 ppm sweep width, 6.1 μs (90°) pulse length, a pulse delay of 2 s, 32 scans, 64K time domain, zero filling to 128K, and slight Gaussian apodization to give enhanced resolution. The basic assignment of the strongly coupled and partly overlapped resonances was performed with the use of selective decoupling experiments, whereas the stereochemical position of protons on the α- or β-face has been established by one-dimensional (1D) difference NOE measurements. 1D NOE experiments were run with a 5 s irradiation time and with saturation of individual lines within the multiplet. NOE difference spectra were obtained by internal subtraction of on- and off-resonance spectra. The crucial NOE enhancements upon saturation of H6″ (β-side) were found for H2′ (5.5%) and H3′ (0.7%). To obtain accurate *J* coupling data and chemical shifts, ^{1}H NMR spectra at all nine temperatures in the range from 275 to 348 K were simulated with a standard computer simulation algorithm, which is integrated into Varian software (VNMR revision 5.3B). The error in $^3J_{HH}$ is smaller than 0.1 Hz as estimated from the comparison of the experimental and simulated spectra (Figure 1).

Conformational Analysis of $^3J_{HH}$. The conformational analysis of the cyclopentane moiety in **1** has been performed with the use of the computer program PSEUROT[10f] which finds the best fit between experimental and calculated $^3J_{HH}$. The input consists of the parameters P_1−P_6 for the generalized Karplus−Altona equation, the λ electronegativities of the four substituents, *A* and *B* parameters, parameters T_b and P_b for the Barfield transmission effect, the experimental $^3J_{HH}$, and the initial guesses of the geometries of the starting conformers and their respective populations. The following λ electronegativity values were used: 0.0 for H, 0.45 for the *C*-aglycon, 1.26 for OH, 0.60 for C1′ and C4′, 0.62 for C2′ and C3′, 0.68 for C5′, and 0.74 for C6′. The magnitude of the Barfield correction on the cisoid $^3J_{1'6'}$, $^3J_{2'3'}$, and $^3J_{4'6'}$ coupling constants depends on the parameters T_b and P_b ($\Delta J = T_b \cos^2\{P - P_b\}$). The parameter T_b is the amplitude of the effect and is 2.0 for carbon, whereas the parameter P_b is the phase angle of pseudorotation of the envelope form at which the maximum is reached.[10g,h] The discrepancy between experimental and calculated $^3J_{HH}$ has been monitored through the calculation of the root-mean-square error. As one of the conformers is populated by less than 20%, we have constrained its geometry during the iteration procedure. To find the global minimum, we have systematically varied input parameters for the major conformer in the following way: P_S was varied in the range from 119° to 154° in 3° steps, and Ψ_m^S was independently varied from 25° to 49° in 3° steps (Figure 4). After finding the geometry of the major conformer which gives the lowest root-mean-square error, we have constrained the major S-type conformer to the optimized geometry and varied P_N in range from 10° to 46° in 6° steps, whereas Ψ_m^N was independently varied from 31° to 52° in 4° steps to improve the agreement between J^{expt} and J^{calcd} (Figure 4). The smallest root-mean-square error and the lowest difference between J^{expt} and J^{calcd} were obtained with $P_N = 28°$ and $\Psi_m^N = 43°$ as the minor conformer, which were in further optimizations of **1** constrained to assume a fixed value when the geometry of the major conformer was optimized. The best fit between J^{expt} and J^{calcd} was obtained with $P_S = 137°$ and $\Psi_m^S = 37°$ (root-mean-square error 0.52 Hz, $\Delta J^{max} < 0.8$ Hz).

Ab Initio MO Calculations. All calculations were performed with the GAUSSIAN 94 program (SGI-G94 Revision D.1)[13] running on a Silicon Graphics Indigo 2 with an R4000 processor and IRIS Power Challenge with four R8000 processors. For all the pseudorotamers all internal degrees of freedom were first freely optimized at the Hartree−Fock (HF) level of theory using the standard 3-21G basis set. For the calculation of the energy profile shown in Figure 2, endocyclic torsion angles ν_2 and ν_3 were kept fixed to scan the conformational space. HF/3-21G optimized geometries of the N-, E-, and S-type conformers were used as input for the completely free geometry optimizations at the HF/6-31G(d) level. In addition energy calculations were performed with inclusion of the electron correlation using the second-order Møller−Plesset (MP2) theory and Becke-style three-parameter hybrid density functional using the Lee−Yang−Parr correlation functional (B3LYP). Stationary points were verified through vibrational frequency calculations. The details of the results of the calculations are given in the Supporting Information.

Acknowledgment. We thank the Ministry of Science and Technology of the Republic of Slovenia (Grants Z1-8609-0104 and COST D2/0002/94) and Krka, Pharmaceutical and Chemical Works, Novo mesto, Slovenia, for financial support and for their financial contribution for the purchase of 300 and 600 MHz Varian NMR spectrometers. We thank one reviewer for the suggestion to run ab initio calculations also at a higher level of theory.

Supporting Information Available: Table listing the selection of bond distances and bond angles from ab initio optimized geometries and Cartesian coordinates and total energies of N, E, and S conformers as archive entries produced by Gaussian 94 (7 pages). See any current masthead page for ordering information and Web access instructions.

JA972433G

(13) Gaussian 94: Frisch, M. J.; Trucks, G. W.; Schlegel, H. B.; Gill, P. M. W.; Johnson, B. G.; Robb, M. A.; Cheeseman, J. R.; Keith, T.; Petersson, G. A.; Montgomery, J. A.; Raghavachari, K.; Al-Laham, M. A.; Zakrzewski, V. G.; Ortiz, J. V.; Foresman, J. B.; Cioslowski, J.; Stefanov, B. B.; Nanayakkara, A.; Challacombe, M.; Peng, C. Y.; Ayala, P. Y.; Chen, W.; Wong, M. W.; Andres, J. L.; Replogle, E. S.; Gomperts, R.; Martin, R. L.; Fox, D. J.; Binkley, J. S.; Defrees, D. J.; Baker, J.; Stewart, J. P.; Head-Gordon, M.; Gonzalez, C.; Pople, J. A., Gaussian, Inc., Pittsburgh, PA, 1995.